Nuclear Instruments and Methods in Physics Research A 632 (2011) 167–174

Contents lists available at ScienceDirect

Nuclear Instruments and Methods in Physics Research A

journal homepage: www.elsevier.com/locate/nima

Reporting detection efficiency for semiconductor neutron detectors: A need for a standard

Douglas S. McGregor *, J. Kenneth Shultis

S.M.A.R.T. Laboratory, Mechanical and Nuclear Engineering Department, Kansas State University, Manhattan, KS 66506, United States

ARTICLE INFO

Article history:
Received 2 December 2010
Accepted 10 December 2010
Available online 17 December 2010

Keywords:
Semiconductor neutron detector
Neutron detection efficiency

ABSTRACT

In the past few years, there has been an increased interest in the development of alternative neutron detection technologies. Included among many promising alternative neutron detection technologies are semiconductor-based neutron detectors. These detectors are typically small and compact, hence those methods used to characterize large gas-filled neutron detectors are inappropriate. Proposed are standard methods that can be used to model the performance of semiconductor neutron detectors and to characterize experimentally the intrinsic efficiency of these detectors.

1. Introduction

Recently there has been great interest in alternative neutron detection technologies motivated by a projected ^{3}He supply shortage and, thus, an inability to produce more ^{3}He gas-tube thermal-neutron detectors. Included among these various alternative neutron detection technologies are solid-state neutron detectors that incorporate a semiconductor in their design. These semiconductor neutron detectors can be divided into two major types, namely coated/perforated diode detectors and solid-form bulk detectors [1].

The basic construction of these alternative devices distinguishes between the two designs. Coated/perforated diode neutron detectors consist of some form of semiconductor rectifying device upon which a neutron reactive coating has been applied to a pn junction diode and/or perforations in the diode are filled with neutron reactive material. Solid-form bulk devices are semiconductor detectors in which one or more constituent elements of the material are neutron reactive, such as CdZnTe and BAs detectors.

These semiconductor devices, produced by various research groups, currently undergo analysis with different modeling and experimental methods. Moreover, a variety of different and *inconsistent* methods are being used for both the modeling and the experimental measurements of detector efficiencies. In many cases, the modeling parameters and methods are vaguely described, unrealistic, or unsubstantiated. Likewise, there is often an information deficit for reported experimentally determined neutron detection efficiencies. Sadly, many reported results, although ambitious and initially impressive, are so vaguely described or different from standard practice that their validity is suspect.

The primary reason for these varied reporting methods is a lack of a standard for (1) modeling the detector response to incident neutrons and (2) measuring properly the neutron detection efficiency. Because several researchers have recently entered this important field, it has become clear that conventions must be agreed upon for the proper modeling of detector response functions and standard methods established for experimentally determining neutron detection efficiencies. Offered in this paper is a standard by which neutron detection efficiencies can be modeled and measured.

2. Efficiency definitions

Depending upon the application, the "efficiency" of a detector can have multiple meanings and can be estimated by a variety of methods. Several different definitions of detector efficiencies are discussed in the following subsections, along with descriptions of some presently used standards for radiation emitted by radioactive point sources. Then efficiency definitions for detectors illuminated by beams of radiation are presented.

2.1. Absolute efficiency

The *absolute efficiency* ε_A is defined as the ratio of the measured number of counts recorded by the detector to the total number of emissions from the radiation source during a time Δt or, equivalently, the ratio of the count rate to the source emission rate, namely

$$\varepsilon_A = \frac{R_{det}}{AB}. \tag{1}$$

Here R_{det} is the count rate, A is the source activity and B is the branching ratio of the radiation emission under investigation, i.e., the probability the radiation of concern is emitted per radioactive decay.

* Corresponding author.
E-mail address: mcgregor@ksu.edu (D.S. McGregor).
URL: http://www.mne.ksu.edu/research/centers/SMARTlab (D.S. McGregor).

0168-9002/$ - see front matter © 2010 Elsevier B.V. All rights reserved.
doi:10.1016/j.nima.2010.12.084

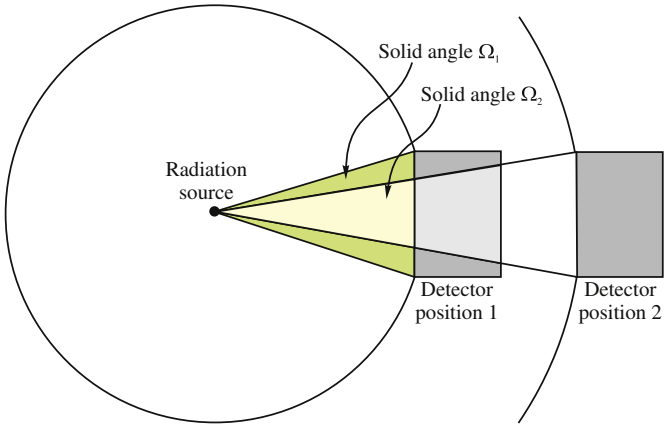

Fig. 1. Absolute efficiency is a function of the detector properties and the source/detector geometry. The radiation flux entering the detector at position 1 is greater than the radiation flux entering the detector at position 2.

The absolute efficiency changes with the source/detector geometric arrangement; hence it has little value if the experimental arrangement is not described with enough specificity to allow the experiment to be reproduced. As shown in Fig. 1, the solid angle subtending the detector in position 1, which is closer to the source, is larger than when the detector is in position 2. Consequently, the expected number of radiation quanta entering the detector at position 1 is greater than that entering the detector in position 2. From Eq. (1), the detector when placed in position 1 has a higher absolute efficiency than when in position 2. Yet the detector has not changed; hence, the absolute efficiency defines the performance of the detector with regard to detector properties *and* geometrical positioning with respect to the radiation source.

For reporting purposes, the absolute efficiency can be useful provided that a standard geometric arrangement is used so that experimenters can use identical conditions to determine this efficiency. For instance, the efficiency performance of high-purity Ge (HPGe) detectors is commonly reported as an absolute efficiency under the guidelines of ANSI/IEEE 325-1996 that prescribes the detector be tested with a NIST-traceable calibrated ^{60}Co source placed exactly 25 cm away from and centered perpendicularly to the working face of the device [2]. Only the 1332-keV gamma-ray peak in the pulse height spectrum is used in the measurement, in which the count rate for the 1332 keV peak is divided by the source activity ($B=1$).

2.2. Relative efficiency

The *relative efficiency* ε_R is the absolute efficiency of a test detector compared directly with another reference detector with a known absolute efficiency ε_A^{ref} under identical irradiation conditions, namely

$$\varepsilon_R = \frac{R_{det}}{AB\varepsilon_A^{ref}}. \tag{2}$$

Typically, the reference detector is an established standard. For instance, for a HPGe detector the ANSI/IEEE 325-1996 standard prescribes that the detector be compared to a 3-in. × 3-in. (7.62-cm × 7.62-cm) right-cylindrical NaI(Tl) detector. Under the ANSI/IEEE 325-1996 guidelines, the established absolute efficiency for a 3-in. × 3-in. right-cylindrical NaI(Tl) detector is 1.2×10^{-3} [2].[1]

[1] Although the authors of Ref. [2] quote *ex cathedra* the efficiency of a 3-in. × 3-in. right-cylindrical NaI(Tl) detector, there is no description in the work as to how this absolute efficiency was obtained, nor the uncertainty associated with the measurement. As a result, the number appears to be somewhat arbitrary, although commonly used, and the relative efficiencies associated with its use are at best consistent.

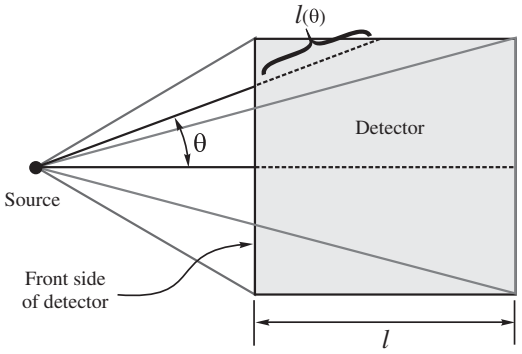

Fig. 2. Intrinsic efficiency can suffer from parallax effects, in which the detector absorber depth l is a function of the radiation intersection angle θ. Here the point source is on the axis of a cylindrical detector.

Commercial vendors commonly quote the relative efficiency for HPGe detectors, which is presumed to be in accordance to the ANSI/IEEE 325-1996 standard.

2.3. Intrinsic efficiency

The *intrinsic efficiency* ε_i is the ratio of the detector response (counts or count rate) R to the particle emission or emission rate divided by the solid angle Ω subtended by the detector from the point source, namely

$$\varepsilon_i = \frac{R_{det}}{AB\Omega}. \tag{3}$$

Here Ω is proportional to the probability that radiation quanta intersect the detector face. The intrinsic efficiency is often reported in an attempt to reduce the dependence of the measured efficiency upon the measurement geometry. If the intrinsic efficiency is reported in terms of percent, then a normalization factor of 4π is introduced, i.e.

$$\%\varepsilon_i = 100\frac{4\pi R_{det}}{AB\Omega}. \tag{4}$$

The quantity $\Omega/4\pi$ is the probability that a source particle hits the detector. Intrinsic efficiency can, thus, be used to scale the expected absolute efficiency for various alternate source/detector geometries.

Although the intrinsic efficiency mitigates the geometric dependence of the efficiency measurement, it does not completely eliminate the geometric dependence. First, if the intrinsic efficiency is measured from a point source, then the parallax of the radiation emissions subtending the detector become important for small source–detector distances, and can introduce appreciable error. Consider the case shown in Fig. 2, in which the absorber length l is a function of the source–detector angle θ. The radiation attenuation, or absorption efficiency, can be generally described by

$$\varepsilon_a(E,\theta) = 1-e^{-\mu(E)l(\theta)} \tag{5}$$

where $\mu(E)$ is the energy dependent attenuation coefficient and $l(\theta)$ is the effective absorber depth in the detector for an intersecting angle θ. The intrinsic efficiency is then given by [3]

$$\varepsilon_i = \frac{\int_0^{\theta_0} A(1-e^{-\mu(E)l(\theta)})\frac{1}{2}\sin\theta\, d\theta}{A\int_0^{\theta_0}\frac{1}{2}\sin\theta\, d\theta} = \frac{\int_0^{\theta_0}\varepsilon_a(E,\theta)\sin\theta\, d\theta}{\int_0^{\theta_0}\sin\theta\, d\theta}. \tag{6}$$

Note that in Eq. (6) it is assumed that a radiation absorption event produces a detectable pulse; hence, this equation generally

overestimates the actual intrinsic efficiency. Further, $\mu(E)$ describes the probability of an interaction occurring, but does not indicate the energy deposited in the detector nor the resulting pulse height. For a simple radiation counter, absorption reactions may generate pulse heights above the lower level discriminator (LLD) setting, hence, all such counts contribute to the response. However, for example, gamma-ray spectrometers require energy information, and only pulses produced within a full energy peak may be of interest. Because gamma rays may interact through small angle scattering, thereby depositing little energy, an interaction may occur that does not contribute to the detector count rate.

2.4. Intrinsic efficiency for a beam of radiation

Of primary concern in this paper are the efficiencies of thermal-neutron detectors. All known neutron sources produce only fast neutrons. To produce an effective point source of thermal neutrons, a fast neutron source must be placed in a moderator and placed sufficiently far from the thermal-neutron detector so that the source-moderator assembly "appears" as a point source. In this case, the thermal-neutrons strike the detector almost as a uniform plane parallel beam.

For a nearly parallel monodirectional radiation beam, as might be expected from a neutron beam port, the solid angle dependence of the intrinsic efficient is small, hence, for the beam normally incident on one face of the detector,

$$\varepsilon_i = \frac{R_{det}}{IM} = \frac{C(1-e^{-\mu(E)l(\theta)})}{IM} \tag{7}$$

where C is a scaling constant, I is the radiation current or intensity (particle flow per unit area perpendicular to the beam), M is the detector area intersected by the radiation beam, and the absorber length $l(\theta)$ is assumed constant because $\theta \approx 0^\circ$. In the case that all absorptions lead to a registered count, the value of C is unity. However, as the LLD is increased, C decreases.

From Eq. (7), a problem with reporting intrinsic efficiency in a radiation beam is apparent. The intrinsic efficiency can change with the intersected area M if the average absorber length l does not change inversely proportional. Consider the case of a coated semiconductor neutron detector shown in Fig. 3a, where it is assumed that the area dimensions are much greater than the detector width W. If a monodirectional neutron beam intersects the broad face of the detector, then the area M is large, but the absorber length l is small. Should the detector be turned on its side, as shown in Fig. 3b, the area M is small, and the absorber length l is large. Hence, unless M and l are perfectly balanced in these two cases, the reported intrinsic efficiencies for the two different orientations can be quite different.

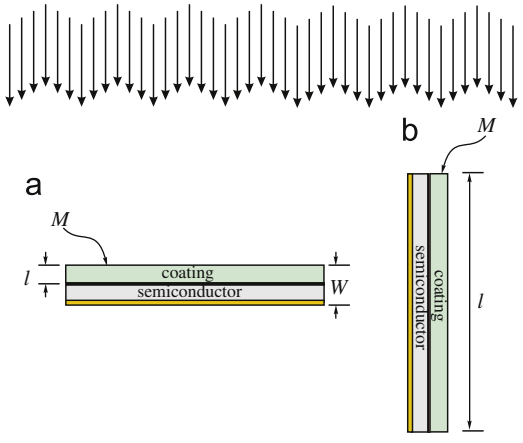

Fig. 3. A coated semiconductor neutron detector with (a) the broad side, denoted the perpendicular case, facing the neutron current and (b) the edge side facing the neutron current.

2.5. Effective intrinsic efficiency in a radiation beam

The *effective intrinsic efficiency* ε_{ei} accounts for solid angle and area effects, as well as a normalization function to correct for various other irradiation angles. The effective intrinsic efficiency is thus defined as

$$\varepsilon_{ei} = \frac{R_{det}M(\theta)}{IM_\perp^2} = \frac{C(1-e^{-\mu(E)l(\theta)})M(\theta)}{IM_\perp^2} \tag{8}$$

where $M_\perp$ is the projected detector area for the perpendicular irradiation case as shown in Fig. 3a and $M(\theta)$ is a projected detector area as a function of θ. As a result, the effective intrinsic efficiency is normalized to the initial irradiation orientation, the perpendicular case. Consider the coated semiconductor neutron detector example of Fig. 3 again. As the detector is rotated from the normal incidence condition, the projected area in the neutron beam reduces approximately by $\cos\theta$. Using the optimum intrinsic efficiency condition for such a detector, described elsewhere [4], the uncorrected intrinsic efficiency and effective intrinsic efficiency are shown for such a device in Fig. 4. Note that the intrinsic efficiency increases as the detector is rotated from normal incidence to 90°; but, when corrected by $\cos\theta$, the actual effective intrinsic efficiency decreases as the detector is rotated from normal to 90°. Because the detector area is decreasing as the detector is rotated from normal incidence, the overall effect is to reduce the count rate and, hence, the effective intrinsic efficiency of the detector is reduced. The effective intrinsic efficiency and area correction factor are important considerations for detectors that are irradiated simultaneously from multiple directions or for detectors that may be turned through various angles during operation.

2.6. Summary

Four different commonly reported detector efficiencies have been described, those being the absolute, relative, intrinsic and effective intrinsic efficiencies. In general, detector efficiencies are quoted for specific source–detector orientations, hence the use of absolute, relative and intrinsic efficiencies can be used provided that they are reported for a standardized source–detector geometry. Use of these reported efficiencies for alternate source–detector

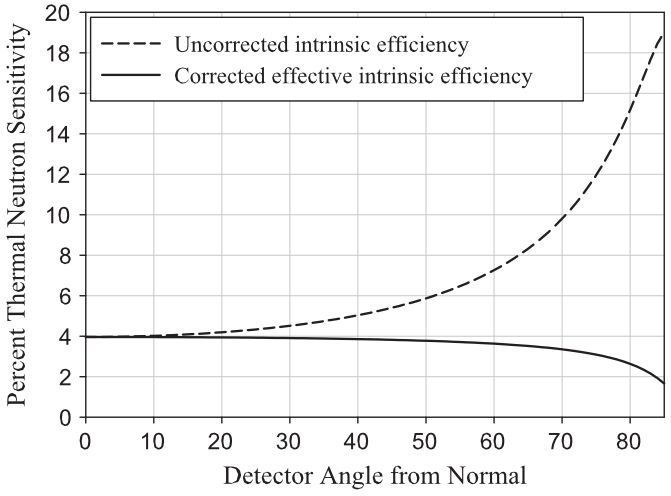

Fig. 4. Calculated intrinsic efficiency and effective intrinsic efficiency for a ^{10}B-coated semiconductor neutron detector. The ^{10}B coating is 2.45 μm thick and the LLD is set at 300 keV equivalent [4].

geometries can result in appreciable error or even non-sensical efficiency calibrations. For angular changes, or for irradiation from multiple angles, the effective intrinsic efficiency, corrected for each angle of incidence, should be used.

Finally, it should be noted that the emission rate of source particles has implicitly been assumed to be constant over the measurement times. This constancy is often hard to realize for neutrons produced by a nuclear reactor in which small drifts in the fission rate can occur, especially if the measurements are made over a period of hours. In such cases, beam-port monitors must be used to correct the measurements for small variations in the beam intensity.

3. Neutron absorber materials and reaction rates

The neutron reaction rate within a detector depends on the neutron flux within the detector. If the neutron flux is known, then the simple ratio between the reaction rate and the flux should yield the detector efficiency. However, there are several factors that can either simplify or complicate the measurement of the detector efficiency. In the following discussion, it is assumed that a mono-directional beam of thermal-neutrons is incident on a neutron absorber.

3.1. 1/v neutron absorbers

Radiative capture of neutrons can be accurately modeled with the Breit–Wigner approximation [5]

$$\sigma_\gamma(E_c) = \pi\lambda_1^2 g\sqrt{\frac{E_1}{E_c}}\frac{\Gamma_n\Gamma_\gamma}{(E_c-E_1)^2+\Gamma^2/4} \tag{9}$$

where E_1 is the energy of the lowest energy resonance, E_c is the center-of-mass between the neutron and target nuclei [5], λ_1 is the reduced wavelength for a particle at energy E_1, Γ_n is the neutron line width, Γ_γ is the radiation line width, Γ is the total decay width, and g is a statistical factor that is a function of the spin of the target and the resulting compound nucleus. Because E_1, λ_1, Γ_n, Γ_γ, Γ are constants, the radiative capture cross section produces a $1/v_c$ behavior at low neutron energies $E_c \ll E_1$, namely

$$\sigma_\gamma(E_c) \approx K_1\sqrt{\frac{E_1}{E_c}} = \frac{K_2}{v_c} \tag{10}$$

where K_1 and K_2 are proportionality constants.

The cross section for neutron capture resulting in the release of charged particles can be expressed by [5]

$$\sigma_{(a,b)} = \sqrt{\frac{E_b}{E_a}}H(E_a) \approx \frac{K_3}{v_a} \tag{11}$$

for the reaction $X(a,b)Y$. Here E_a and E_b are the kinetic energies of the particles in the center-of-mass system and $H(E_a)$ is a correction factor for non-$1/v$ behavior for moderately large $E_a < E_1$, and K_3 is a proportionality constant. Neutrons at low energy $E_a \ll E_1$ have little effect on the reaction Q value, so the Q value of the reaction is nearly equal to E_b. In such cases $H(E_a) \approx 1$. Shown in Fig. 5 are the $1/v$ absorption cross sections for the common neutron detector absorber materials ^{3}He, ^{10}B, and ^{6}Li, all of which release charged particle reaction products upon absorption of a thermal neutron.

3.2. Non-1/v absorbers

There are numerous absorbers used for neutron detectors that do not exhibit $1/v_c$ behavior, usually due to resonances appearing in the epithermal and thermal-neutron range. These materials include

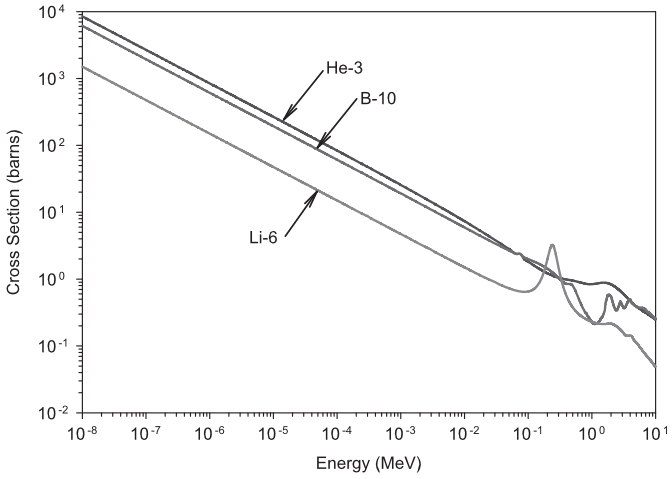

Fig. 5. Neutron absorption cross sections in barns for common $1/v$ neutron detector materials [6]. The energy is the incident neutron energy in the center-of-mass coordinate system.

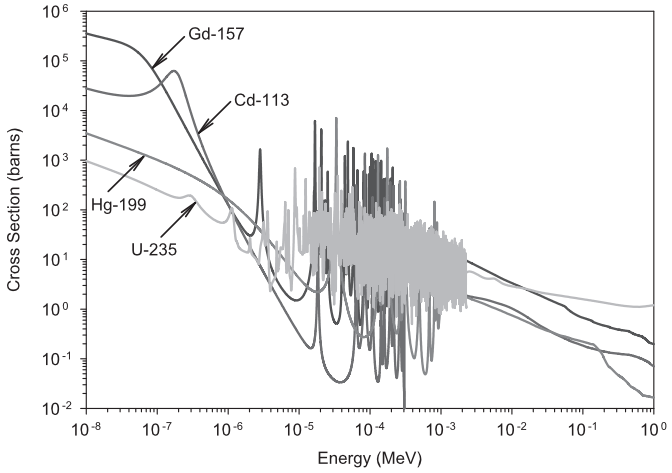

Fig. 6. Neutron absorption cross sections in barns for common non-$1/v$ neutron detector materials [6], showing the radiative capture cross sections for ^{113}Cd, ^{157}Gd and ^{199}Hg, and the fission cross section for ^{235}U. For such heavy nuclide targets the center-of-mass neutron energy almost equals the neutron energy in the laboratory system.

^{113}Cd, ^{157}Gd, ^{199}Hg and ^{235}U. The energy dependent cross sections for these alternative neutron detector materials are shown in Fig. 6.

3.3. Reaction rates in the 1/v region

Consider the laboratory system where neutrons approach target nuclei with relative velocities

$$\mathbf{v}_r = \mathbf{v} - \mathbf{V} \tag{12}$$

where $\mathbf{v}$ is the neutron velocity vector and $\mathbf{V}$ is the target nuclei velocity vector. As observed from the target nuclei, the incident neutrons are a differential beam of intensity

$$dI = n(\mathbf{v})v_r\, d\mathbf{v} \tag{13}$$

where $n(\mathbf{v})$ is the neutron density distribution and

$$v_r = |\mathbf{v}_r|. \tag{14}$$

The neutrons interact with the nuclei at a density rate

$$dF = n(\mathbf{v})N(\mathbf{V})\sigma(v_r)v_r\, d\mathbf{v}\, d\mathbf{V}\ (\mathrm{cm}^{-3}\ \mathrm{s}^{-1}) \tag{15}$$

where $N(\mathbf{V})$ is the target nuclei velocity density distribution and $\sigma(v_r)$ is the neutron cross section at the relative speed v_r. The total

interaction rate density is then

$$F = \iint (n\mathbf{v})N(\mathbf{V})\sigma(v_r)v_r \, d\mathbf{v} \, d\mathbf{V}. \tag{16}$$

If the target nuclei exhibit $1/v_r$ absorption behavior, then from Eqs. (10) and (11), any arbitrary cross section $\sigma(v_{ro})$ for relative speed v_{ro} is related to the cross section at v_r by

$$\sigma(v_r) = \frac{\sigma(v_{ro})v_{ro}}{v_r}. \tag{17}$$

Substitution of Eq. (17) into Eq. (16) yields

$$\begin{aligned} F &= \iint n(\mathbf{v})N(\mathbf{V})\sigma(v_r)v_r \, d\mathbf{v} \, d\mathbf{V} \\ &= \iint n(\mathbf{v})N(\mathbf{V})\frac{\sigma(v_{ro})v_{ro}}{v_r}v_r \, d\mathbf{v} \, d\mathbf{V} \\ &= N\sigma_a(v_{ro})nv_{ro} = \Sigma_a(E_0)nv_0 \end{aligned} \tag{18}$$

where $\Sigma_a(E_0)$ is an arbitrarily chosen macroscopic reaction cross section at corresponding speed v_o, n is the total neutron density, and N is the total target nuclei density. The result of Eq. (18) is very important, and states that the reaction rate of neutrons with a $1/v$ material is independent of the neutron or target nuclei velocity distributions! Hence, a measurement using a reaction rate to determine detection efficiency is independent of the neutron energy distribution for $1/v$ absorbers. In the case that the absorber nuclei are non-$1/v$, a thermally dependent Westcott correction factor $g_a(T)$ is required to correct for non-$1/v$ interaction behavior [5], i.e.

$$F = g_a(T)\Sigma_a(E_0)nv_0, \tag{19}$$

where T is the neutron temperature of the assumed Maxwellian spectrum of the incident neutrons.

4. Methods used to calibrate neutron detectors

There are numerous methods used by credible organizations to calibrate and determine "efficiency" of neutron detectors. Yet, these calibration methods differ significantly and, hence, do not provide a reliable standard by which neutron detection efficiencies can be reported, especially for small thermal-neutron semiconductor detectors. Described in the following sections are a few of these calibration methods, although they do not represent the plethora of methods used by various other organizations. Unfortunately, these different measurement protocals, although mostly reproducible, are often not easily related to each other.

Note that, according to NIST [10], (1) there is no reliable method to produce an omnidirectional thermal-neutron source to test a detector in an isotropic flux and (2) the MCNP code can be used to understand the experimental conditions and optimize a measurement but it is inadequate for efficiency calibrations. For instance, a 5% uncertainty in the code output, along with a 5% uncertainty in the neutron measurement, results in unacceptable error in the neutron efficiency calibration for NIST-traceable detectors. Further, using a ^{252}Cf source moderated with a high-density polyethylene (HDPE) ball requires correction for albedo neutrons scattering in the room, a correction that can be accomplished by backing the detector away and measuring the deviation in the point-source response.

4.1. Reuter-Stokes method

Reuter-Stokes, a major manufacturer of neutron detection instrumentation, uses a compact method to calibrate their products [7]. The method is used to provide a general approximation of the thermal-neutron detection efficiency.

A large box formed by walls of 6 in. thick high-density polyethylene (HDPE) is used as a moderator. The box has a large open cavity in the center. A neutron source, such as ^{252}Cf, is inserted in the box, centered near one of the walls. Gold activation foils are used to measure the thermal-neutron flux at locations throughout the box after making neutron self-absorption corrections for the foils. Thus, the neutron flux is thoroughly mapped throughout the box. A detector is then placed in the box, at an angle, near the wall opposite that near the neutron source. Counts are taken with the detector, correcting for the spatial differences in neutron flux. The results are periodically checked against a NIST calibrated detector. The resulting measurements yield relative efficiencies as compared to a NIST-traceable standard. However, it is not clear how corrections are made for perturbations in the thermal-neutron flux spatial distribution in the box caused by the foils or detector.

Hence, the Reuter-Stokes method relies upon a fast neutron source moderated in a box that produces a thermal-neutron flux incident on the detector from nearly 4π directions. Due to the nature of the source–detector configuration, the neutron flux intersecting the detector is not uniform in direction or space. Yet, the Au foil calibration allows approximate corrections to be made. Overall, the Reuter-Stokes method might be adequate for large gas-filled detectors to provide a measure of ε_i. Note that the Reuter-Stokes method is clearly an "in-house" technique, and would be difficult to reproduce elsewhere. Further, due to uncertainties in the neutron flux density and energy distribution at small spatial scales, this method seems inappropriate for smaller semiconductor thermal-neutron detectors.

4.2. ORNL method

One of the many methods used at Oak Ridge National Laboratory (ORNL), home of the Spallation Neutron Source (SNS), also uses a moderated ^{252}Cf source [8,9]. The neutron source is placed within a large block of HDPE capable of moderating and minimizing the leakage of neutrons. A beam port has been drilled into the HDPE block oriented towards the source that still leaves enough moderator in the port to produce a thermalized neutron beam. A borated shutter, composed of x–y direction jaws, is attached to the moderator block around the beam port and is used to reduce the beam cross section. The thermal-neutron flux at the testing location is measured with a calibrated neutron detector. For additional verification, MCNP is used to calculate the expected neutron flux and profile at the testing location, quoted as having approximately 10% error. The count rate of the experimental detectors per unit area is then divided by the measured thermal-neutron flux to determine the intrinsic neutron detection efficiency.

4.3. NIST method

The National Institute of Standards and Technology (NIST) uses a combination of a calibrated neutron current and calibrated neutron detectors to determine the unknown efficiency of a neutron detector [10]. The calibration consists of using a ^{252}Cf neutron source placed in a heavy-water moderator pool, which works to approximate the environment inside a light-water reactor.

However, the preferred method for testing a thermal-neutron detector is with a single-crystal diffracted beam, whose spatial profile is determined from activation analysis of a Dy foil, or is measured with a neutron-imaging detector. Hence, the neutron beam profile is documented within the work space. The neutron flux is measured by "trusted" fission chambers calibrated in the past. Hence, the basic method is to (1) profile the relative thermal-

neutron beam intensity as a function of position and then (2) measure the neutron current (or fluence) with a calibrated standard fission chamber. The count rate of the unknown detector is then directly compared with the measured neutron current, as described in Eq. (7). Note that fission chambers, typically fabricated with U as the neutron reactive material, deviate slightly from the ideal $1/v$ behavior. Hence, knowledge of the diffraction angle, and resulting neutron energy, is important for thermal corrections to the NIST calibration method.

4.4. KSU method

The method used at Kansas State University (KSU) eliminates the need for a calibrated neutron detector or a calibrated neutron beam. Hence, the technique can be used to determine the intrinsic efficiency for a test detector, such as a ^{3}He detector, that can then be used as a standard for future calibration measurements of experimental semiconductor neutron detectors [11].

A diffracted neutron beam from the Kansas State University TRIGA Mark II nuclear reactor is used for the efficiency calibrations. The beam diffraction angle is set to deliver a beam of approximately 0.0253 eV thermalized neutrons to the work space, chosen because it is the most probable energy in a thermalized Maxwellian distribution at room temperature. The undiffracted neutron beam is shielded with 4 ft of concrete, behind which is a beam catcher filled with borated HDPE. The diffracted neutron beam is stopped down to a diameter of 1.27 cm with a cadmium shutter. The work area is lined with 2 in. thick borated HPDE. Another beam catcher filled with borated HPDE is placed in line with the diffracted neutron beam beyond the work area to capture the monoenergetic neutron beam. These precautions reduce leakage and albedo neutron contamination in the work area to minimal levels. The basic experimental arrangement is shown in Fig. 7.

A 2-in. diameter, 6-in. long, Reuter-Stokes model P4-1603-207, ^{3}He detector is used as a test detector. The device has a 35-mil-thick (889 μm) 304-stainless-steel shell, which can absorb approximately 10% of the 0.0253 eV diffracted neutron beam. Because the ^{3}He detector has long field tubes at each end, there are appreciable dead regions at each end of the detector. The ^{3}He detector is laid sideways and centered in the neutron beam, such that the beam intersects perpendicular to the axis of the detector (not along the long axis), to measure the relative attenuation of the beam as it passes through the tube (see Fig. 8). The relatively large diameter of the ^{3}He reference detector, being much larger than the neutron beam diameter, reduces curvature effects that might otherwise confuse the neutron absorption component of the metal container. A BF_3 neutron detector is placed behind the ^{3}He detector as the reference detector. The diffracted neutron beam as it passes through the stainless-steel walls and the ^{3}He gas produces a count rate in the BF_3 detector

$$R_{out} = R_{in} e^{-\Sigma_w t_w} e^{-\Sigma_g t_g} e^{-\Sigma_w t_w} = R_{in} e^{-2\Sigma_w t_w} e^{-\Sigma_g t_g} \tag{20}$$

where R_{in} is the neutron count rate before attenuation through the ^{3}He detector, R_{out} is the neutron count rate after attenuation through the ^{3}He detector, Σ_w is the macroscopic cross section of the ^{3}He detector stainless-steel tube, Σ_g is the macroscopic cross section of the ^{3}He gas, t_w is the thickness of the ^{3}He detector stainless-steel tube wall, and t_g is the inner diameter of the ^{3}He gas detector. The transmission factor for the ^{3}He detector is

$$T_d = e^{-2\Sigma_w t_w} e^{-\sigma_g t_g} = \frac{R_{out}}{R_{in}}. \tag{21}$$

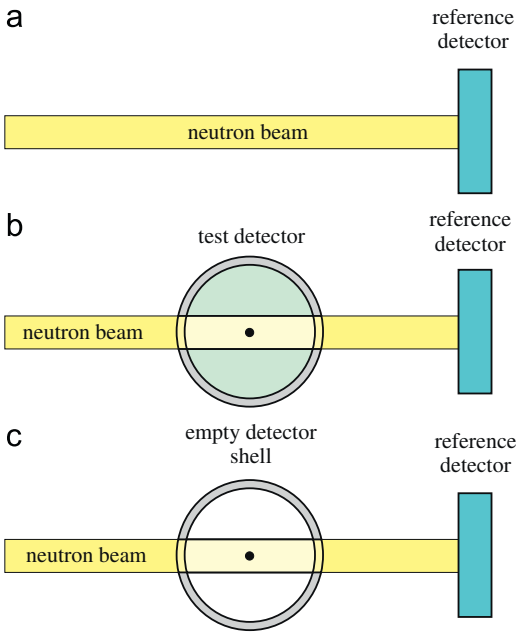

Fig. 8. KSU calibration method for determining the efficiency of a test detector. After the calibration, the test detector can be used as a calibration standard for other experimental neutron detectors. A 1/v detector, such as the BF_3 detector mentioned in the text, is used as the reference detector.

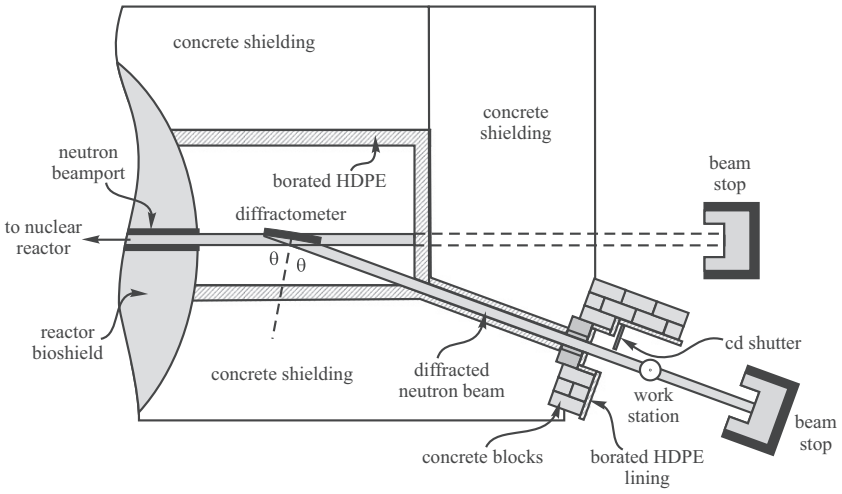

Fig. 7. Basic experimental arrangement used at KSU to calibrate neutron detectors. Neutrons are incident on diffractometer from TRIGA Mark II nuclear reactor.

Hence, T_d yields the attenuation through both the detector shell and the ^{3}He gas in the test detector. With the assumption that two inches of air has little effect on the neutron beam attenuation, the ^{3}He detector shell transmission factor was determined by placing an empty 304-stainless-steel tube casing, with the same steel-thickness and radius of the ^{3}He gas detector, in the beam, and by measuring the transmission factor,

$$T_{2w} = e^{-2\Sigma_w t_w} = \frac{R_w}{R_{in}} \tag{22}$$

where R_w is the count rate from the beam attenuated by the empty stainless-steel-tube casing. It is assumed that the gas of the ^{3}He detector is the sensitive volume and attenuation in the gas accounts for all neutron counts produced by the detector. Conversely, it is also assumed that any additional attenuation in the steel casing does not contribute to counts. The transmission factor of the detector gas is determined by substituting Eq. (22) into Eq. (21) to yield

$$T_g = \frac{R_{out}}{R_w} = e^{-\Sigma_g t_g}. \tag{23}$$

The fraction of the beam attenuated by the gas in the detector reveals the fraction of interactions in the ^{3}He, yet it does not yield directly the detector efficiency. The beam that is attenuated in the ^{3}He gas was already attenuated by a single thickness of the steel casing. Hence, the fraction of the beam that is transmitted through one thickness of the sheet metal is

$$T_{1w} = e^{-\Sigma_w t_w} = [e^{-2\Sigma_w t_w}]^{1/2} = \sqrt{\frac{R_w}{R_{in}}}. \tag{24}$$

Because the efficiency is determined by neutrons absorbed in the ^{3}He gas, the ^{3}He detector efficiency is

$$\varepsilon_g = \frac{\sigma_{ao}}{\sigma_{to}} e^{-\Sigma_w t_w}(1 - e^{-\Sigma_g t_g}) \tag{25}$$

where σ_{ao} is the absorption cross section leading to detectable events and σ_{to} is the total cross section at energy E_o. The total cross section σ_{to} is the total probability that a neutron will interact with a target nuclei, including capture, fission, elastic scattering, and inelastic scattering. Because inelastic and elastic scattering usually do not follow a $1/v$ dependence, the ratio σ_{ao}/σ_{to} deviates from $1/v$ behavior at moderately high neutron energies, and proper corrections must be made to account for these differences. However, in the low energy $1/v$ range, generally below 10 eV, $\sigma_{ao} \approx \sigma_{to}$; therefore substitution of Eqs. (23) and (24) into Eq. (25) yields

$$\varepsilon_g = \sqrt{\frac{R_w}{R_{in}}}\left(1 - \frac{R_{out}}{R_w}\right) \tag{26}$$

which is the intrinsic detection efficiency for the ^{3}He detector when intersected by the 1.27 cm diameter beam. Hence, provided that other detectors are calibrated with the same beam area, the ^{3}He detector can be used as a standard detector for relative measurements to provide the intrinsic neutron detection efficiency of experimental devices. Note that, for simplicity, all calibration measurements are performed for identical time durations Δt. This same calibration method can be used for neutron detectors based upon ^{10}B and ^{6}Li materials. The count rates R_{in}, R_{out}, and R_w are independent of each other; hence the uncertainty associated with the measured intrinsic efficiency, as a function of these count rates, can be easily determined through error propagation. Further, the measurements can be designed so as to reduce the experimental error below 1%.

Because both ^{3}He and $^{10}BF_3$ are $1/v$ absorbers and the diffracted neutrons are within the $1/v$ energy range, the neutron energy is not needed to obtain the intrinsic detection efficiency with this calibration method. Further, even if the neutrons were not mono-energetic and were spread over a Maxwellian or other energy distribution, information of the neutron energies is still not needed, provided that the spectrum of energies is within the $1/v$ region. Note that stainless steel, the construction material for the ^{3}He detector container, is a non-$1/v$ material, yet the thickness of the container absorbs few neutrons, hence the non-$1/v$ factor has little effect on the measurement.[2]

From the discussion in section 3, the count rates represented by R_{in}, R_{out}, and R_w are independent of neutron energy for materials with $1/v$ cross sections. Corrections may also apply for $1/v$ absorbers, because of the σ_{ao}/σ_{to} ratio, if the neutrons in the beam have energies exceeding approximately 10 eV; therefore thorough moderation is required. Finally, if the detector under test is composed of non-$1/v$ absorbers for the neutron reactive material, such as ^{157}Gd, ^{113}Cd or ^{235}U, then it is necessary to apply the appropriate non-$1/v$ corrections to the calculated efficiency.

5. Conclusion

Semiconductor neutron detectors are generally designed with a preferred orientation facing the neutron source. Given this preference, the authors recommend that modeling of such detectors be performed under the condition that a parallel monodirection current of neutrons strikes orthogonal to the preferred detector face. Such an analysis removes ambiguous calculations that use unrealistic "isotropic" flux conditions, and allows straightforward experimental verification.

The most desired arrangement to determine neutron detection efficiency is a diffracted neutron beam from a nuclear reactor. The diffracted beam is removed from fast neutron and gamma-ray background radiations. Further, for the case of non-$1/v$ neutron detectors, the known energy of the diffracted beam permits easy efficiency and count rate corrections for other neutron energies. It is recommended that the diffracted beam be collimated to a work location that has been shielded to reduce albedo neutron contamination. Finally, the test location should allow the experimenter to place the preferred detector orientation orthogonal in the neutron beam to reproduce the recommended modeling conditions.

From the discussion in Section 3, a research group that does not have access to a nuclear reactor can build a simple experimental measurement system with ^{252}Cf, AmBe or PuBe sources, provided that

(1) the neutrons are adequately thermalized down into the low $1/v$ region,
(2) albedo neutron contamination is reduced or eliminated,
(3) the standard reference detector used to calibrate the neutron current is a $1/v$ detector, such as ^{3}He or $^{10}BF_3$ gas-filled detectors, and
(4) the experimental detectors and encapsulates are composed of $1/v$ materials.

The authors recommend that the KSU efficiency calibration method be adopted, mainly because it (1) removes the initial need for a calibrated reference detector, (2) allows the experimenters to determine the efficiency of their reference detector with less than 1% error, (3) can be easily modeled for design optimization and response function calculations, and (4) provides a standard

[2] The total neutron cross sections of Fe, Cr and Ni, the predominant elements in 304 stainless steel, are dominated by elastic scattering. Further, the elastic scattering cross sections are constant from thermal energies up to at least 70 eV for all three elements. The neutron capture cross sections are $1/v$, with Westcott correction factors (at 0.0253 eV) $g_a = 0.993$ for Fe and $g_a = 1.00$ for Cr and Ni [12]. Hence, any $1/v$ neutron absorptions have little effect on the measurement, and any scattering uniformly removes neutrons of all energies below 70 eV. Overall, the stainless-steel container has almost no effect on the calibration.

measurement method that can be repeated by other research groups exploring innovative semiconductor neutron detectors.

As a final note, it might be argued that detectors in moderator boxes or pools do not experience the same conditions as devices in a monodirectional beam. However, the vast number of different moderator configurations used for thermal-neutron detectors make it nearly impossible to report the results from these numerous geometries. Use of the thermalized uncollided neutron current to measure the efficiency does provide a standard value by which the expected performance for other detector configurations, including moderated detector configurations, can be calculated.

Acknowledgements

The authors express gratitude to Zane Bell and Ron Cooper of ORNL, Nathan Johnson and David O'Connor of GE Reuter Stokes, and Alan Thompson of NIST for helpful discussions.

References

[1] D.S. McGregor, J.K. Shultis, Nucl. Instr. and Meth. A 517 (2004) 180.
[2] E. Fairstein, S. Wagner, et al., IEEE Standard Test Procedures for Germanium Gamma-Ray Detectors, IEEE Std 325-1996, NIDC, 1996.
[3] N. Tsoulfanidis, Measurement and Detection of Radiation, second ed., Taylor and Francis, Washington, 1995.
[4] D.S. McGregor, M.D. Hammig, H.K. Gersch, Y.-H. Yang, R.T. Klann, Nucl. Instr. and Meth. A 500 (2003) 272.
[5] J.R. Lamarsh, Nuclear Reactor Theory, Addison-Wesley, Reading, 1966.
[6] ENDFPLOT-2, Korea Atomic Energy Research Institute, 〈http://atom.kaeri.re.kr/endfplot.shtml〉, 2010.
[7] N. Johnson, GE Reuter-Stokes, private communication, 2010.
[8] Z. Bell, Oak Ridge National Laboratory, private communication, 2010.
[9] R. Cooper, Oak Ridge National Laboratory, private communication, 2010.
[10] A. Thompson, National Institute of Standards and Technology, private communication, 2010.
[11] D.S. McGregor, W.J. McNeil, S.L. Bellinger, T.C. Unruh, J.K. Shultis, Nucl. Instr. and Meth. A 608 (2009) 125.
[12] T. Nakagawa, et al., J. Nucl. Sci. Technol. 32 (1995) 1259.